# Next-generation all-solid-state battery (#ASSB)

Tuan Vo<sup>a,b†</sup>, Claas Hüter<sup>b</sup>, Stefanie Braun<sup>a</sup>, Manuel Torrilhon<sup>a</sup>

<sup>a</sup>Department of Mathematics, Applied and Computational Mathematics (ACoM), RWTH Aachen University, Schinkelstraße 02, 52062 Aachen, Germany <sup>b</sup>Institute of Energy and Climate Research (IEK-2), Forschungszentrum Jülich, Wilhelm-Johnen-Straße, 52428 Jülich, Germany

## Mathematical modelling for the next-generation All-solid-state batteries: Nucleation (SE|SSE)<sup>(\*)</sup>-interface

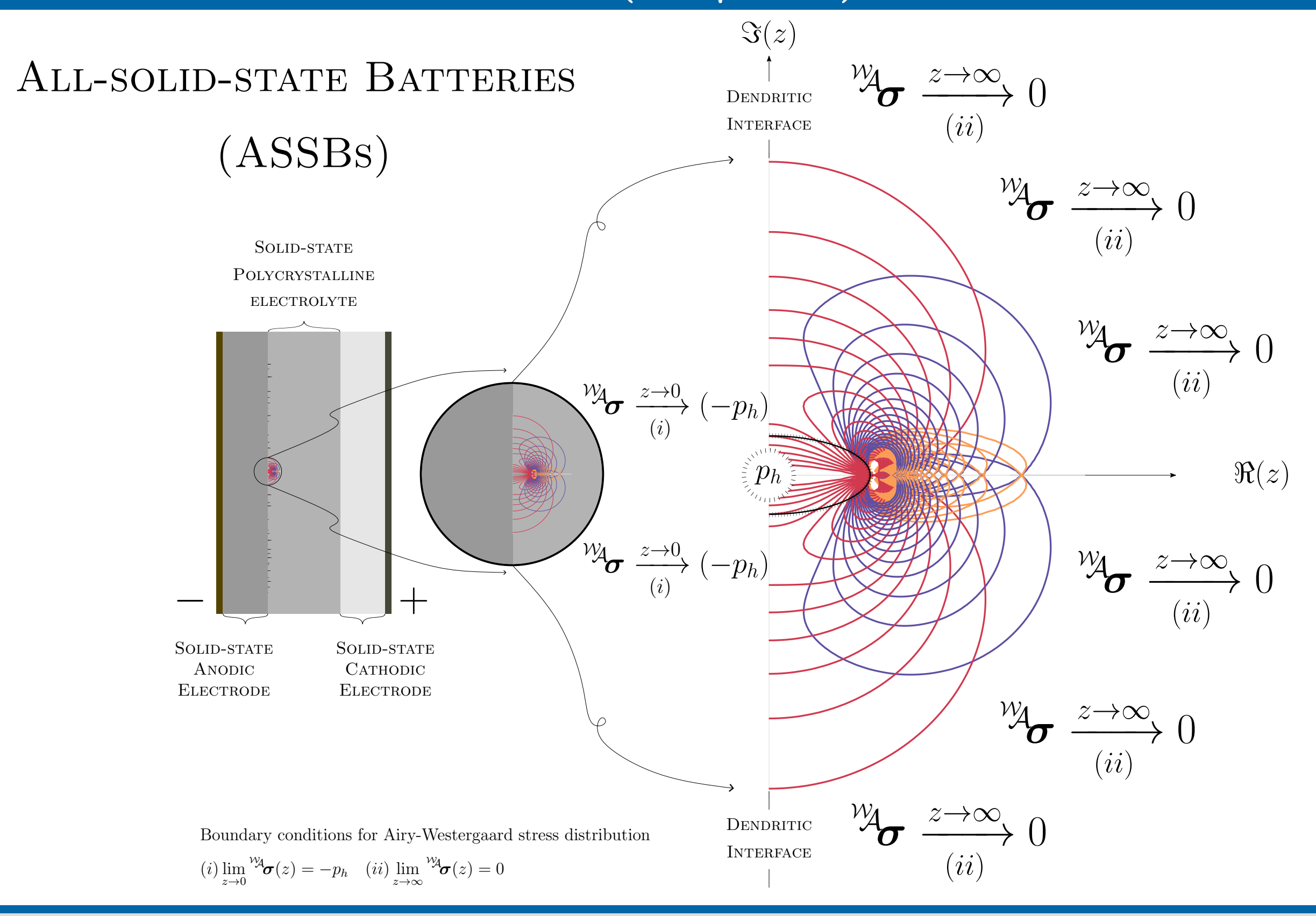
Rechargeable Lithium-ion battery (LIB) is at the heart of every electric vehicle (EV), portable electronic device, and energy storage system [1]. Nowadays, LIBs enable human life more efficient and help to solve global environment issues thanks to EVs' zero emission. However, conventional LIB (c-LIB) is sensible to temperature and pressure, hence, flammable and explosive, which is undesirable. This bottleneck is mainly due to liquid-based electrolyte found in c-LIBs.

**All-solid-state battery** (ASSB) is one of promising candidates to overcome bottlenecks of c-LIBs. Thanks to solid-state electrolyte (SSE), ASSB is highly stable towards temperature and pressure. Nevertheless, Limetal dendrite triggered at (SE|SSE)-interface [5] is the main drawback of ASSB since these dendritic threads extrapolate into SSE grain boundary network, causing crevice, degradation of ionic conductivity, and the probability of short-circuit, which is unfavorable.

**Next-generation All-solid-state battery** (ng-ASSB) with a consideration of nucleation criterion defined by

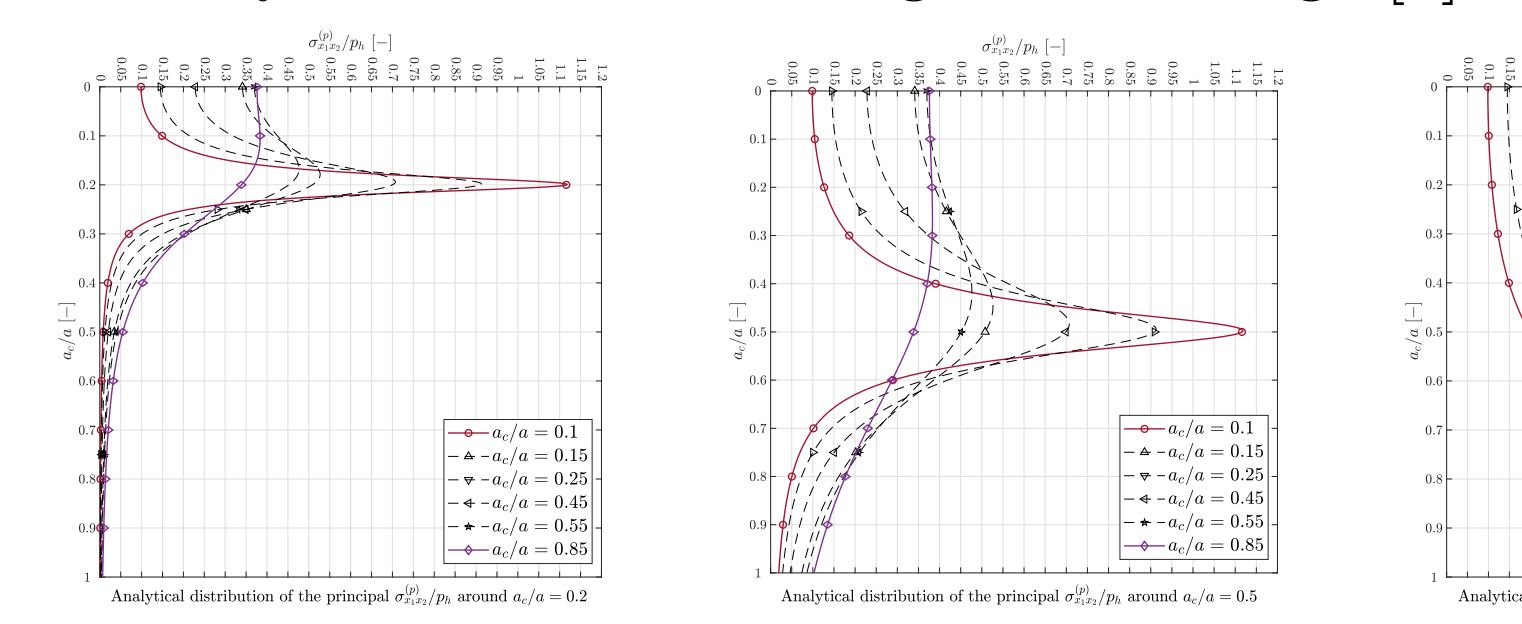
$$a_{ ext{Griffith}} := a^* = \arg\min_{a \in \mathbb{R}} \left. \iint_{\Omega} f(a, \boldsymbol{u}, \theta; \lambda, \mu, \boldsymbol{d}^R \otimes \boldsymbol{d}^R) \, d\Omega - \iint_{\Gamma} f(a; \gamma) \, d\Gamma \right|_{\boldsymbol{u}^{(k)}}$$

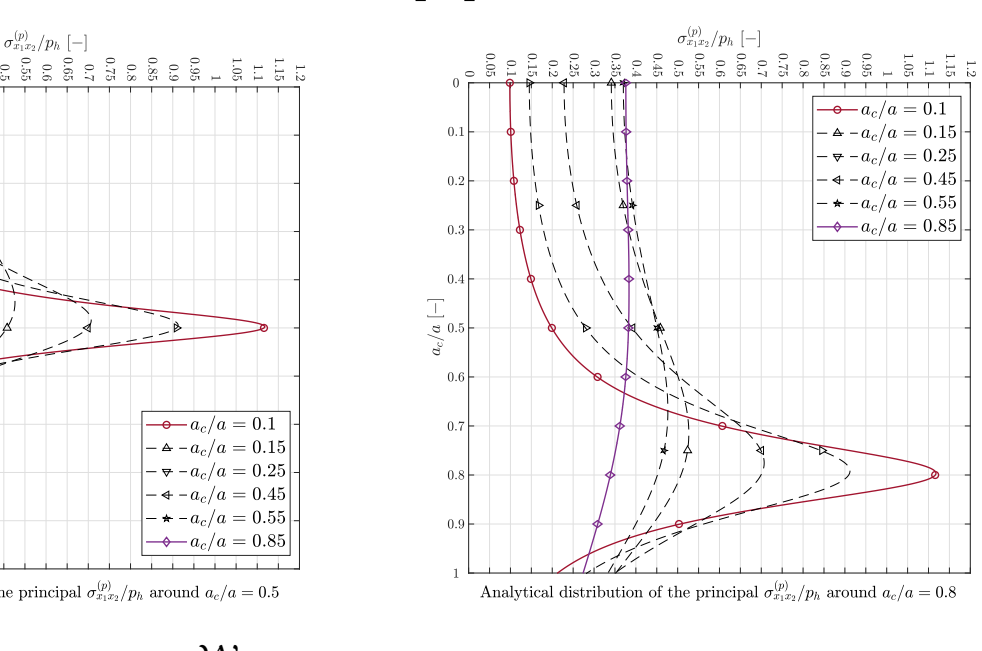
where  $\boldsymbol{u}$  displacement field,  $\theta$  temperature field, a crevice length,  $\lambda, \mu$  Lamé constants,  $\boldsymbol{d}^R \otimes \boldsymbol{d}^R$  embedded misorientation structural tensor, and  $\gamma$  cracking-surface energy density, can help to improve ASSB performance.



## Interface Analysis

Interface between solid electrode and solid-state electrolyte (SE|SSE) taking place at space charge layer (SCL) [2] found in ASSBs critically exhibits mechanical and electrochemical instability [3]. This evidence points directly to the fact that the soft metallic li anode is erroneously prone to triggering dendrites, under cycles of electric charge & discharge [5].

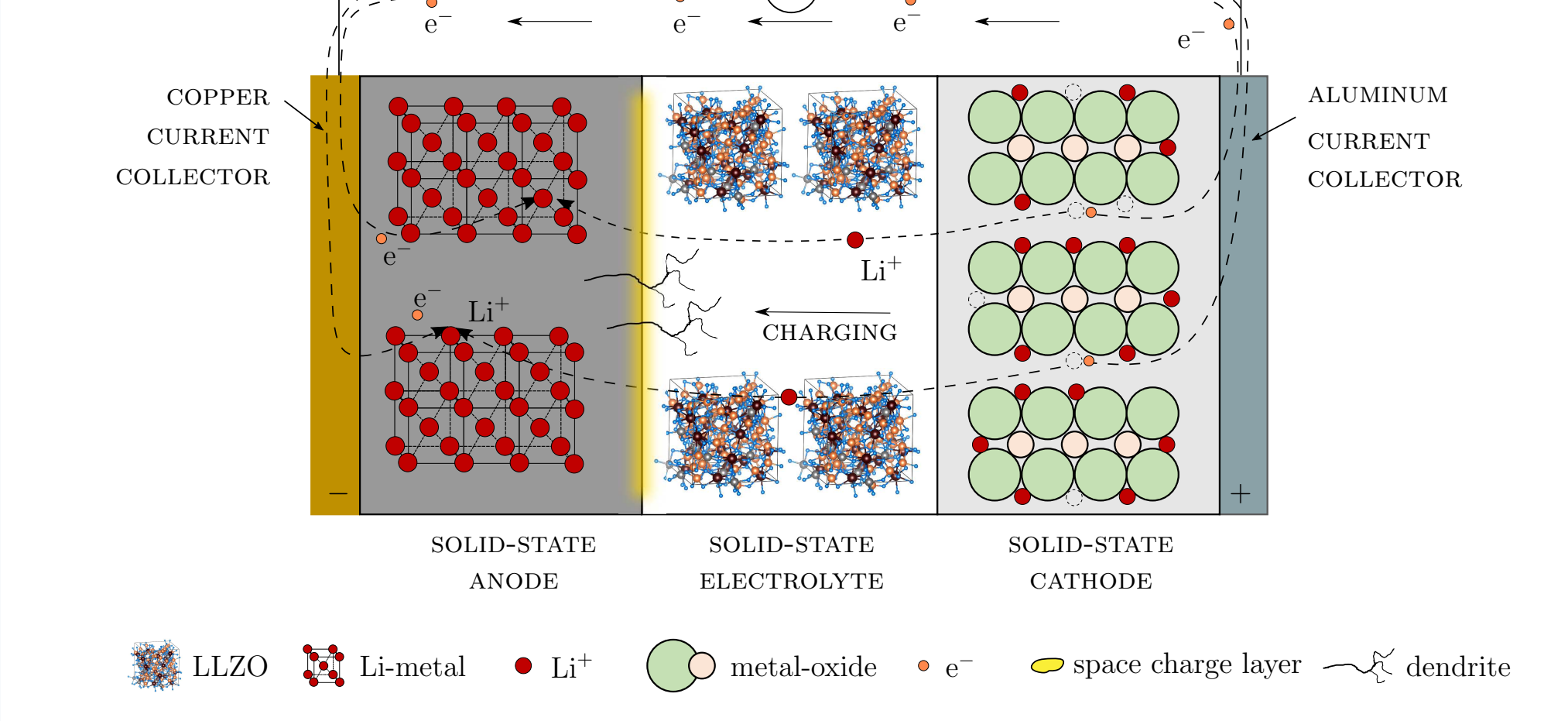




<u>Distribution</u>: ana. max. shear stress  ${}^{\mathcal{W}}\!\!\sigma_{x_1x_2}^{\Pi}$  around crack tip  $a_c$ .

## Next-generation All-solid-state battery

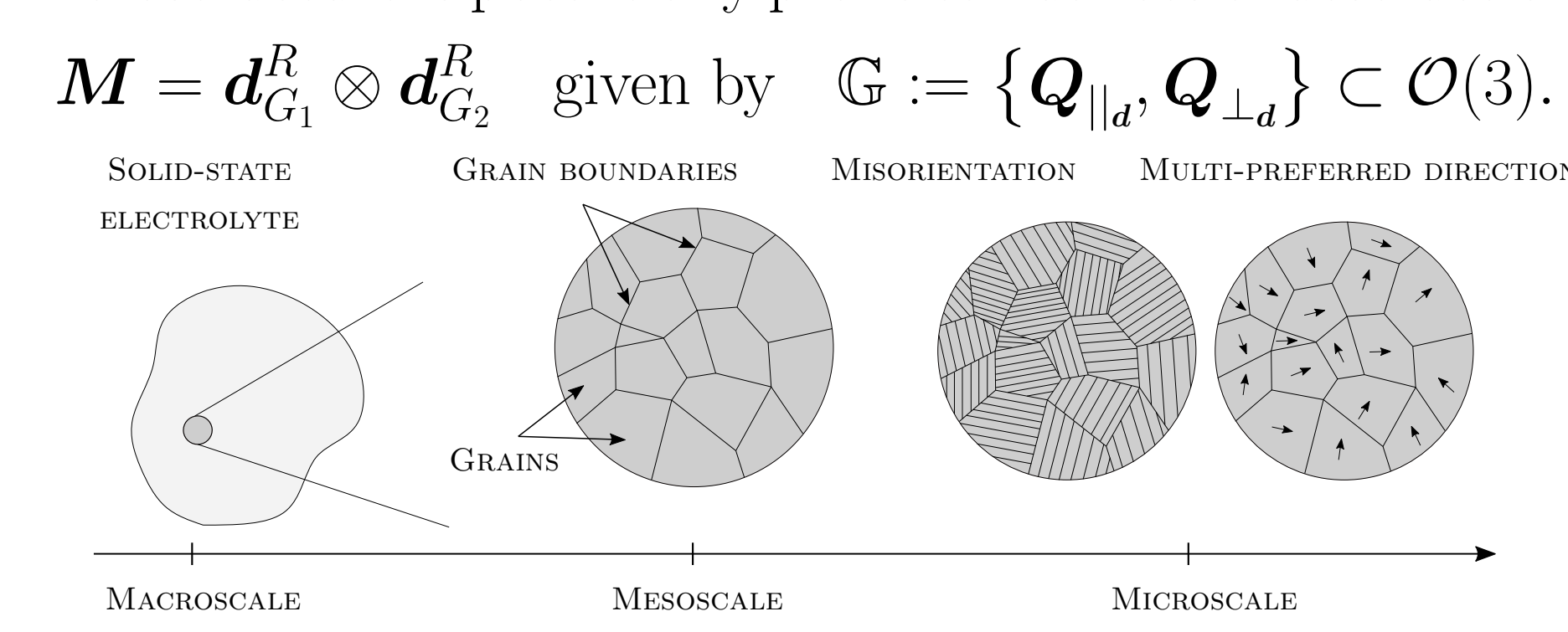
**Nucleation** criterion governs the instable (SE|SSE)-interface [3]



**Thermodynamic consistency** is satisfied, followed by [2]. ✓ Closure  $\bar{\Omega}$  is fulfilled by 15 moments, followed by [4].

## Embedded structural-tensor in SSE

Polycrystalline garnet-type SSE [5] such as LLZO exhibit grain boundary network, and grains with variation of {size, shape} under microscopic observation. Hence, this microstructure is potentially prone to nuances of destruction.



Consequentially, dendrites contribute to degradation of ionic conductivity and tiny-cracks tracing along grain boundaries.

## Nucleation interface: Taking place at the critical dendritic interface

Coupled fields: Displacement field  $\boldsymbol{u}$  and temperature field  $\boldsymbol{\theta}$ ; structural tensor  $\boldsymbol{M}$ 

$$oxed{oxed} oxed{u}: egin{cases} \Omega imes \mathbb{R}_+ 
ightarrow \mathbb{R}^3, \ (oldsymbol{x},t) \mapsto oldsymbol{u}(oldsymbol{x},t), \end{cases} egin{aligned} heta: egin{cases} \Omega imes \mathbb{R}_+ 
ightarrow \mathbb{R}, \ (oldsymbol{x},t) \mapsto heta(oldsymbol{x},t), \end{cases} oxed{M}_{i=1,...,N}^{\{RR,RE\}}: egin{cases} oldsymbol{d}_{ ext{Grain i}}^R \otimes oldsymbol{d}_{ ext{Grain i}}^R \\ oldsymbol{d}_{ ext{Grain i}}^R \otimes oldsymbol{d}_{ ext{Grain i}}^R \end{cases}$$

Governing conservation equations

$$\frac{d}{dt} \int_{\Omega} (\cdot) \ d\Omega = \int_{\Omega} (\cdot)^{\text{action}} \ d\Omega + \int_{\partial \Omega} (\cdot)^{\text{action}} \ d\partial\Omega + \int_{\Omega} (\cdot)^{\text{production (+/-)}} \ d\Omega$$

 $\rho(\boldsymbol{x},t)$  is mass density per unit volume (puv);  $\boldsymbol{b}(\boldsymbol{x},t)$  body force puv;  $\boldsymbol{v}(\boldsymbol{x},t)$  velocity;  $e(\boldsymbol{x},t)$  internal energy puv;  $\boldsymbol{q}(\boldsymbol{x},t)$  heat flux;  $r(\boldsymbol{x},t)$  heat source puv;  $\boldsymbol{\sigma}$  Cauchy stress and  $\varepsilon$  infinitesimal strain. Helmholtz energy functional

$$a_{\text{Griffith}} := a^* = \arg\min_{a \in \mathbb{R}} \left. \iint_{\Omega} f(a, \boldsymbol{u}; \lambda, \mu, \boldsymbol{d} \otimes \boldsymbol{d}) \, d\Omega - \left. \iint_{\Gamma} f(a; \gamma) \, d\Gamma \right|_{\boldsymbol{u}^{(s)}}$$

Governing PDE

$$a_{ ext{Griffith}} := a^* = \arg\min_{a \in \mathbb{R}} \left. \iint_{\Omega} f(a, \boldsymbol{u}; \lambda, \mu, \boldsymbol{d} \otimes \boldsymbol{d}) \, d\Omega - \left. \iint_{\Gamma} f(a; \gamma) \, d\Gamma \right|_{\boldsymbol{u}^{(s)}}$$

Strain energy: Interface between solid solid-state electrolyte electrode and (SE|SSE) taking place at space charge

 $\iiint_{\Omega} f(a, \boldsymbol{u}; \lambda, \mu, \boldsymbol{d} \otimes \boldsymbol{d}) d\Omega$ 

Interface between Surface energy: solid electrode and solid-state electrolyte (SE|SSE) taking place

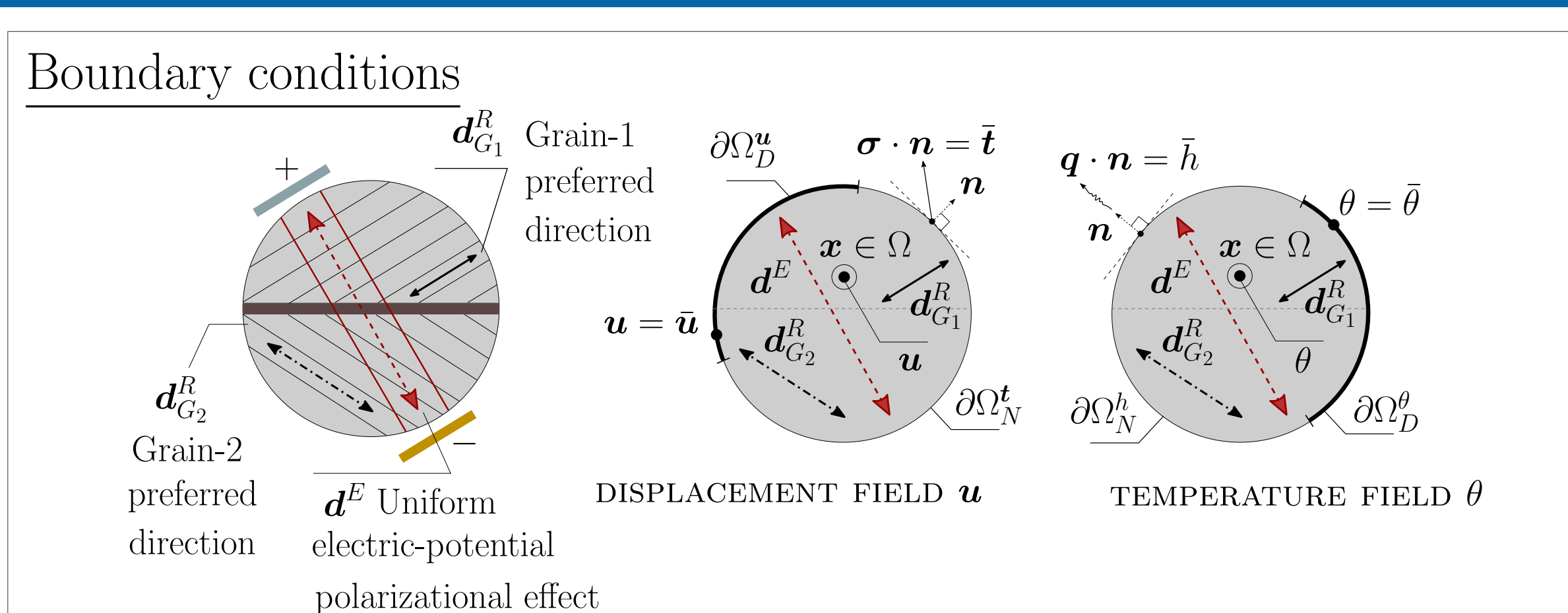
$$\iint_{\Gamma} f(a;\gamma) \, d\Gamma$$

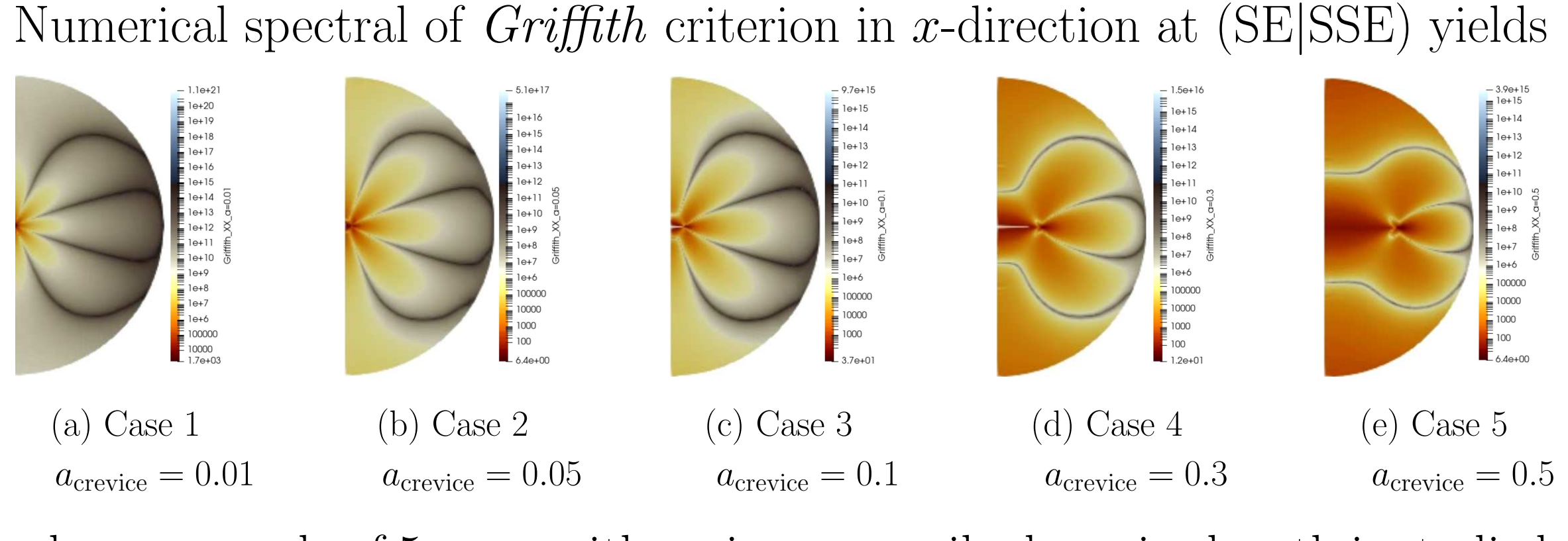
Therefore, the governing problem of dendritic nucleation at (SE|SSE) takes the form

$$\partial_t oldsymbol{u} + 
abla \cdot \left( \overset{4}{\mathbb{C}}^{f_{ ext{alocation}}(\lambda, \mu, oldsymbol{d}_{G_i, i=1,...,N}^R, oldsymbol{d}^E; oldsymbol{x})} : 
abla oldsymbol{u}^{(s)} 
ight) + 
ho oldsymbol{b} = -
ho 
abla V_e,$$

s.t. 
$$a_{\text{Griffith}} := a^* = \arg\min_{a \in \mathbb{R}} \iiint_{\Omega} f(a, \boldsymbol{u}, \theta; \lambda, \mu, \boldsymbol{d} \otimes \boldsymbol{d}) d\Omega - \iint_{\Gamma} f(a; \gamma) d\Gamma \Big|_{\bar{\boldsymbol{u}}}$$

where





where a sample of 5 cases with various prescribed crevice length is studied.

 $abla \cdot \left( \overset{4}{\mathbb{C}} f^{\mathbb{D}(\Omega)}_{(\lambda,\mu)} \, 
abla^{(s)} oldsymbol{u} 
ight) + 
ho \, oldsymbol{b} = oldsymbol{0}$ Displacement vector field solution  $oldsymbol{u_i} \leftarrow oldsymbol{u} = oldsymbol{K}^{-1} oldsymbol{f}$ Strain tensor  $\varepsilon_{ij} = \frac{1}{2} \left( \partial_{x_i} u_i + \partial_{x_i} u_j \right)$ Stress tensor  $\sigma_{ij} = \sum_{k,l} \overset{4}{\mathbb{C}}_{(\lambda,\mu)}^{f_{(\lambda,\mu)}^{\mathbb{D}}} \, arepsilon_{kl}$ 

Strain energy density

 $\mathcal{E}_{ ext{strain}} := rac{1}{2} \sum_{i,j} \sigma_{ij} \, \varepsilon_{ij}$ 

FEM: Strain energy density

Partial differential equation (PDE)

Analysis: Airy-Westergaard function used for stress analysis: (i) max. shear stress and (ii) principal stresses

$$\mathcal{Y}_{\mathcal{A}} : \begin{cases} \mathbb{C} \to \mathbb{C}, \\ z \mapsto \mathcal{Y}_{\mathcal{A}}(z) := \Re(\oint_{\Gamma} \mathcal{K}^{(\star)} dz) + x_2 \Im(\oint_{\Gamma} \mathcal{K}^{(\star)} dz), \end{cases} \mathcal{K}^{(\star)} : \begin{cases} \mathbb{C} \to \mathbb{C}, \\ z \mapsto \mathcal{K}^{(\star)} := -p_h + p_h/\sqrt{1 - a^2/z^2}, \end{cases}$$

where a the crevice length,  $p_h$  pressure at the opening crevice on dendritic interface, and  $\forall \{p_h, a\} \in \mathbb{R}_+$ .

<u>Numerics</u>  $\rightarrow$  <u>FEM</u>: element matrix  $\mathbf{K}^e$  approx. by *Gauss quadrature*; indices imply 4 + 2 = 6 for-loop:  $K_{ik}^{e^{\alpha\beta}} = \int_{\Omega^{\epsilon}} \left( \mathcal{L}_{1}^{\alpha} \, \mathbb{C}_{i1k1}^{fGL}(\boldsymbol{x}) \, \mathcal{R}_{1}^{\beta} + \mathcal{L}_{1}^{\alpha} \, \mathbb{C}_{i1k2}^{fGL}(\boldsymbol{x}) \, \mathcal{R}_{2}^{\beta} + \mathcal{L}_{2}^{\alpha} \, \mathbb{C}_{i2k1}^{fGL}(\boldsymbol{x}) \, \mathcal{R}_{1}^{\beta} + \mathcal{L}_{2}^{\alpha} \, \mathbb{C}_{i2k2}^{fGL}(\boldsymbol{x}) \, \mathcal{R}_{2}^{\beta} \right) \det(\boldsymbol{J}) \, d\Omega^{\xi}$ 

where  $\mathcal{L}_i^{\alpha}$  and  $\mathcal{R}_l^{\beta}$  are gradients of basis functions at node  $\alpha^{th}$  and  $\beta^{th}$ , respectively.

#### Contact

Tuan Vo vo@acom.rwth-aachen.de



References [1] **T.Vo**, Modeling the swelling phenomena of li-ion batt. cells based on a numerical chemo-mech. coupled approach. MA, Robert Bosch Battery Systems GmbH, **2018**.

[2] S.Braun, C. Yada and A. Latz, Thermodynamically consistent model for Space-Charge-Layer formation in a solid electrolyte. Ir. Phys. Chem., 119, 22281-22288, 2015.

[3] **C.Hüter**, S.Fu, M.Finsterbusch, E.Figgemeier, L.Wells, and R.Spatschek, *Electrode-electrolyte interface stability in solid state electrolyte system: influence of* coating thickness under varying residual stresses. AIMS Materials Science, 4(4):867-877, **2017**.

- [4] **M.Torrilhon**. Modeling nonequilibrium gas flow based on moment equations. Annual Review of Fluid Mechanics, 48(1):429-458, **2016**.
- [5] **S.Kim**, J.S.Kim, L.Miara, Y.Wang, S.K.Jung, S.Y.Park, Z.Song, H.King, M.Badding, J.M.Chang, V.Roev, G.Yoon, R.Kim, J.H.Kim, K.Yoon, D.Im, and K.Kang, High-energy and durable li metal batt. using garnet-type solid electrolytes with tailored li-metal compatibility. Nature Communications, 13(1):1883, 2022.







